Available online at www.sciencedirect.com

ScienceDirect

Journal of Nutritional Biochemistry 124 (2024) 109503

Journal of Nutritional Biochemistry

RESEARCH PAPER

Thioredoxin domain containing 5 is involved in the hepatic storage of squalene into lipid droplets in a sex-specific way

Javier Sánchez-Marco[a], Seyed Hesamoddin Bidooki[a,b], Roubi Abuobeid[a], Cristina Barranquero[a,b,c], Tania Herrero-Continente[a], Carmen Arnal[b,d], Roberto Martínez-Beamonte[a,b,c], Roberto Lasheras[e], Joaquín C. Surra[b,c,f], María A. Navarro[a,b,c], María J. Rodríguez-Yoldi[b,c,g], Manuel Arruebo[h,i,j], Victor Sebastian[h,i,j], Jesús Osada[a,b,c,*]

[a] Departamento de Bioquímica y Biología Molecular y Celular, Facultad de Veterinaria, Instituto de Investigación Sanitaria de Aragón-Universidad de Zaragoza, Zaragoza, Spain
[b] Instituto Agroalimentario de Aragón, CITA-Universidad de Zaragoza, Zaragoza, Spain
[c] Centro de Investigación Biomédica en Red de Fisiopatología de la Obesidad y Nutrición (CIBEROBN), Instituto de Salud Carlos III, Madrid, Spain
[d] Departamento de Patología Animal, Facultad de Veterinaria, Instituto de Investigación Sanitaria de Aragón-Universidad de Zaragoza, Zaragoza, Spain
[e] Laboratorio Agroambiental, Servicio de Seguridad Agroalimentaria de la Dirección General de Alimentación y Fomento Agroalimentario, Gobierno de Aragón, Zaragoza, Spain
[f] Departamento de Producción Animal y Ciencia de los Alimentos, Escuela Politécnica Superior de Huesca, Instituto de Investigación Sanitaria de Aragón-Universidad de Zaragoza, Huesca, Spain
[g] Departamento de Farmacología, Fisiología, Medicina Legal y Forense, Facultad de Veterinaria, Instituto de Investigación Sanitaria de Aragón-Universidad de Zaragoza, Zaragoza, Spain
[h] Departamento de Ingeniería Química y Tecnologías del Medio Ambiente, Universidad de Zaragoza, Zaragoza, Spain
[i] Instituto de Nanociencia y Materiales de Aragón (INMA), CSIC-Universidad de Zaragoza, Zaragoza, Spain
[j] Centro de Investigación Biomédica en Red de Bioingeniería, Biomateriales y Nanomedicina (CIBER-BBN), Instituto de Salud Carlos III, Madrid, Spain

Received 20 June 2023; received in revised form 5 October 2023; accepted 23 October 2023

Abstract

Hepatic thioredoxin domain-containing 5 (TXNDC5) is a member of the protein disulfide isomerase family found associated with anti-steatotic properties of squalene and located in the endoplasmic reticulum and in lipid droplets. Considering that the latter are involved in hepatic squalene accumulation, the present research was aimed to investigate the role of TXNDC5 on hepatic squalene management in mice and in the AML12 hepatic cell line. Wild-type and TXNDC5-deficient (KO) mice were fed Western diets with or without 1% squalene supplementation for 6 weeks. In males, but not in females, absence of TXNDC5 blocked hepatic, but not duodenal, squalene accumulation. Hepatic lipid droplets were isolated and characterized using label-free LC-MS/MS analysis. TXNDC5 accumulated in this subcellular compartment of mice receiving squalene and was absent in TXNDC5-KO male mice. The latter mice were unable to store squalene in lipid droplets. CALR and APMAP were some of the proteins that responded to the squalene administration in all studied conditions. CALR and APMAP were positively associated with lipid droplets in the presence of squalene and they were decreased by the absence of TXNDC5. The increased squalene content was reproduced *in vitro* using AML12 cells incubated with squalene-loaded nanoparticles and this effect was not observed in an engineered cell line lacking TXNDC5. The phenomenon was also present when incubated in the presence of a squalene epoxidase inhibitor, suggesting a mechanism of squalene exocytosis involving CALR and APMAP. In conclusion, squalene accumulation in hepatic lipid droplets is sex-dependent on TXNDC5 that blocks its secretion.

Keywords: Olive oil; liver; squalene; TXNDC5; lipid droplets.

1. Introduction

The Mediterranean diet has been associated with a wide range of benefits on cardiovascular health and its associated pathologies such as diabetes, dyslipidemia, hypertension, metabolic syndrome, and obesity. It has also been associated with a lower incidence of neurodegenerative disorders, particularly Alzheimer's disease [1] and may positively influence all-age-related diseases and longevity [2]. This dietary pattern consists of varied plant-based food sources such as fruits, vegetables, virgin olive oil, and nuts

Abbreviations: ER, endoplasmic reticulum; LD, lipid droplets; TG, triacylglycerol; TXNDC5, thioredoxin domain containing 5.

* Corresponding author at: Miguel Servet, 177, Zaragoza, E-50013, Spain. Tel.: +34-976-761-644; fax: +34-976-761-612.
E-mail address: josada@unizar.es (J. Osada).

https://doi.org/10.1016/j.jnutbio.2023.109503

[3]. In fact, virgin olive oil, its main source of fat, has been associated with a reduced risk of general and cause-specific mortality as well [4]. Virgin olive oil, as a fruit juice, is a complex mixture of monounsaturated fatty acid-containing triglycerides and other biologically active substances named minor components and encompassing chemical categories such as hydrocarbons, terpenes, phytosterols and phenolic compounds [5]. The biological effects of the minor components have lately been the focus of attention [6–8].

Hydrocarbons account for about 50% of the unsaponifiable fraction of virgin olive oil representing squalene almost 90% of all the hydrocarbons present [9]. Characterized as an isoprenoid, squalene is an intermediary in the plant biosynthesis of phytosterols and terpenes and animal cholesterol [8]. This isoprenoid has shown antioxidant [10], anti-inflammatory [11], anti-atherosclerotic [12] and tumor-protective properties [13]. Our group found that a high squalene dose decreased hepatic fat content in a sex-dependent manner [12] and that modified the hepatic mitochondrial and microsomal proteomes [14,15] of *Apoe*-deficient mice on a chow diet. Using this experimental animal model on a Western diet, administration of squalene resulted in a decrease in hepatic triglycerides in males, but not in females [16]. Squalene was found to be accumulated in lipid droplets depending on the animal model used [17].

Lipid droplets (LDs) are cytoplasmic organelles characterized by a neutral lipid core of triacylglycerol (TG), cholesteryl esters and retinyl esters surrounded by a monolayer of phospholipids, non-esterified cholesterol and associated proteins. They are involved in lipid metabolism, signal transduction, protein storage and lipid trafficking [for reviews see [18,19]] and play a pivotal role in the lipid accumulation during fatty liver diseases [20,21]. They are also involved in squalene accumulation [17], which may involve changes in their proteome composition. Thioredoxin domain-containing 5 (TXNDC5), located in the endoplasmic reticulum, is a member of the protein disulfide isomerase family [22], which is also present in lipid droplets [23]. Hepatic TXNDC5 levels were found to be negatively associated with fat content in mice fed a squalene-containing diet [14]. Thus, its deficiency may also affect the loading of squalene into lipid droplets and alter their proteome. To address these hypotheses regarding the effect of dietary squalene and to gain more insight into the mechanisms involved, dietary squalene supplementation was carried out in wild-type (WT) and *Txndc5*-deficient (KO) mice of both sexes fed a Western diet. Hepatic LDs were isolated and their proteomic changes investigated by gel LC-MS/MS analysis. In order to distinguish the effects of squalene administration alone, experiments were also performed in WT and *Txndc5*-KO hepatic cell lines.

2. Experimental procedures

2.1. Animals and diets

Two-month-old wild-type and *Txndc5*-deficient mice on C57BL/6J genetic background were generated by crossing heterozygous animals harboring a deletion of exon 3 of *Txndc5* gene and characterized as described [24]. They were housed in sterile filter-top cages on a 12-hour light/12-hour dark cycle at the *Centro de Investigación Biomédica de Aragón*. Mouse experiments were carried out in accordance with the EU Directive 2010/63 on the protection of animals used for scientific purposes, and the study protocol was approved by the Ethics Committee for Animal Research of the University of Zaragoza (PI35/18 and PI03/21).

Four groups ($n = 6$ or 7) for each sex were established: wild-type and *Txndc5*-deficient mice received a purified Western diet with or without 1% squalene. All diets were prepared in our facilities, lyophilized, and stored at −20°C until use. The composition adapted to AIN-93 purified diets for rodents [25] is shown in Supplementary Table 1. Mice had *ad libitum* access to food and water. Intake and body weights were monitored weekly. At the end of the 6-week dietary intervention, food was withdrawn for 16 h, and the mice were weighed, suffocated in a CO_2 chamber and sacrificed. Blood samples were drawn by cardiac puncture, centrifuged at 3,000 *g* for 10 min to obtain plasma or serum. The livers were obtained and excised; most of the pieces were frozen in liquid N_2 and stored at −80 °C until processing, except an aliquot which was stored in buffered formaldehyde.

2.2. Isolation of lipid droplets

They were isolated according to the protocol of Ontko et al. [26]. Briefly, pooled livers of two mice (100 mg), three preparations per experimental condition, were homogenized in 3 mL of 65% sucrose solution with both protease and phosphatase inhibitor cocktails (Roche, Mannheim, Germany) at 4°C. Discontinuous sucrose gradients were prepared as follows: 3 mL of liver homogenates in 65% sucrose were pipetted at the bottom of the centrifuge tubes kept on an ice bath. Then 2 mL of 60% sucrose solution were slowly added, followed by 2 mL of 52% sucrose, 2 mL of 44% sucrose and 2 mL of distilled water. The tubes containing gradients were centrifuged at 25,000 × *g* for 30 min at 4°C and the bands containing the different lipid droplets were collected and refloated on a fresh gradient. The purified bands were collected, an aliquot was saved, and the rest mixed with 3 volumes of acetone and kept at −80 °C for 10 min and then at −20 °C overnight. The tubes were centrifuged at 15,000 × *g* for 15 min at 4°C. The pellets were washed three times, firstly with acetone: diethyl ether 1:1 and then twice with diethyl ether. Dry pellets were resuspended in PBS containing 0.2% Triton X-100 and 10% glycerol and centrifuged 10 min at 15,000 × *g* in order to remove insoluble proteins. Protein concentrations were determined by BioRad dye binding assay (Hercules, CA, USA).

2.3. Sample preparation for mass spectrometry

The proteomic analysis was performed at the Proteomics Unit of Complutense University (Madrid, Spain). Protein samples (150 μg) were loaded onto a 10% SDS-PAGE gel, run until the loading dye reached the separating gel and visualized with G-250 Coomassie blue protein stain (Merck, Darmstadt, Germany). Protein bands were excised for subsequent in gel digestion. Briefly, the proteins were reduced with 10 mM dithiothreitol at 56°C for 30 min, and then alkylated with 25 mM iodoacetamide for 20 min. Finally, proteins were digested with recombinant trypsin (ratio enzyme: protein 1:50, Roche, Mannheim, Germany) in 100 mM ammonium bicarbonate (pH 8.5) overnight at 37°C. Tryptic peptides were extracted in two steps by incubating the gel pieces with 0.1% trifluoroacetic acid and 80% acetonitrile (ACN) for at least 30 min. A final extraction was performed using 100% ACN. The resulting extracts of each sample were combined, dried, dissolved in 2% ACN, 0.1% formic acid (FA) and frozen until analysis.

2.4. LC-MS/MS of lipid droplet proteins

Peptides were analyzed by nano-liquid chromatography (nano Easy-nLC 1000, Thermo Scientific, Bremen, Germany) coupled to a Q-Exactive HF high-resolution mass spectrometer (Thermo Scientific). Peptides were resolved using multi-dimensional capillary LC through an Acclaim PepMap column C18 100 (Thermo Scientific, #164567) connected to a PepMap 100 C18 (Thermo Scientific, #164534) with an integrated spray tip. Separation conditions were a flow rate of 250 nl/min and 160 min linear gradient from 0%

to 45% *v*/v buffer A (0.1% FA in water) and buffer B (0.1% FA in ACN). Peptides were electrospray ionized with a voltage of 1.8 kV at 290°C. The mass spectrometer operated in data-dependent acquisition mode and peptides were detected in full scan MS mode with a resolution of 60,000 and a m/z range of 350–1800 Da. The 15 most intense multiply charged ions were sequentially fragmented by high collision dissociation with a normalized energy of 20%. MS/MS spectra were acquired in positive mode in an information dependent mode with a resolution of 30,000. Raw data were processed using Proteome Discoverer 2.4 (Thermo Scientific) with search engine MASCOT 2.6 (MatrixScience, London, UK) to identify peptides against contaminant database (247 sequences) and *Mus musculus* (strain C57BL/6J) proteome (UP000000589), downloaded from Uniprot (www.uniprot.org). Search parameters included a precursor mass tolerance of 10 ppm and a fragment mass tolerance of 0.02 Da, up to 2 skipped breakpoints allowed for trypsin hydrolysis, carbamidomethyl cysteine as a fixed modification and methionine oxidation, loss of methionine, or loss of methionine plus acetylation of the amino terminus as variable modifications. The relative extracted ion chromatograms (EICs) for each identified protein were filtered accordingly to have at least one unique identified peptide and a false discovery rate (FDR) <0.01. Proteins with an observed EIC in ≤ 1 sample across all samples were removed. The normalized spectral abundance factor (NSAF) for each protein was calculated according to McIlwain et al. [27]. Adopting these criteria, the number of proteins and peptides identified, eliminating contaminants, in each of the male samples is summarized in Supplementary Table 2. A complete description of the proteins with their NSAF can be found in Supplementary Table 3.

2.5. Mass spectrometry data analysis and network analysis

To simplify and reduce the number of proteins, a series of filters such as number of peptides, Mascot index indicating presence, percentage of coverage and Mascot score (Supplementary Fig. 1) were applied. As a result, 297 proteins were compared among the different conditions and only those experiencing a change expressed as $\log_2$ NSAF ratio <-1 or >1 were selected. Those chosen proteins were submitted to the Search Tool for the Retrieval of Interacting Genes (STRING 11.5) website and their KEGG pathways and their networks generated using the high confidence view (score 0.900).

2.6. Western blotting and immunostaining of membranes

Hepatic homogenate or lipid droplet proteins (5 μg) were loaded onto SDS-polyacrylamide gels, electrophoresed, transferred to PVDF membranes and blocked as previously described [28]. The primary antibodies, diluted in PBS buffer containing 2.5% BSA and 1% Tween 20, were added and the membranes were incubated 2 h at room temperature and then overnight at 4°C. The following primary antibodies, with their working dilutions, were used: Rabbit polyclonal antibody against TXNDC5 (1:1,000, Proteintech #19834-1-AP, Manchester, UK), anti-CALR (1:1,000, Proteintech #10292-1-AP). and anti-APMAP (1:2,000, Proteintech #25953-1-AP). Equal loadings were confirmed by using a mouse monoclonal anti-β-ACTIN (1:2,000, Sigma #A5441, St Louis, MO, USA). Membranes were washed three times with a PBS buffer containing 0.1% Tween 20 and incubated for 1 h at room temperature with conjugated goat anti-rabbit IgG (H&L) DyLight 800 secondary antibody (SA5-35571) or goat anti-mice IgG (H&L) DyLight 680 secondary antibody (SA5-35518), both from Thermo-scientific (Waltham, MA, USA), diluted 1:80,000. Images were captured using an Odyssey®-Clx (LI-COR, Bad Homburg, Germany).

2.7. Histological analysis

The portion of the liver stored in formaldehyde was paraffin-embedded and sectioned. Sections were then stained with hematoxylin and eosin, scanned, and scored for lipid droplet area, inflammation, necrosis, and fibrosis by trained histologists blinded to the experimental groups. The lipid droplet areas were estimated in sections with Adobe Photoshop CS3 (Adobe Inc. San Jose, CA, USA) and expressed as percentage of total liver section as previously described [12].

2.8. Hepatic lipids

Lipids were extracted and cholesterol and triglyceride measured as previously described [28] using Infinity Reagent kits from Thermo Scientific (Thermo Fisher Scientific Waltham, MA, USA).

2.9. Squalene quantification

Squalene was extracted and measured as previously published [17].

2.10. RNA isolation and RT-qPCR analysis

Livers were homogenized using Tri Reagent from Ambion (Life Technologies, Carlsbad, CA, USA) and total RNA was extracted using spin column kit Direct-zol RNA Miniprep (Zymo Research, Irvine, CA, USA), following the manufacturer's instructions. RNA was quantified by absorbance at $A_{260/280}$ using Nanodrop Spectrophotometer (Thermo) and the ratio was greater than 1.75 as well as the ratio $A_{260/230}$. The integrity of the 28S and 18S ribosomal RNAs was verified by 1% agarose gel electrophoresis followed by ethidium bromide staining with a ratio 28S/18S greater than 2. Primer design (Supplementary Table 4), RT and cDNA synthesis were carried out as previously described [29]. ViiA7 Real-Time PCR System (Life Technologies) was used, and relative amount of mRNA was calculated using the comparative $2^{-\Delta\Delta Cq}$ method and normalized to the reference *Ppib* expressions.

2.11. Cell culture

The control mouse hepatocyte cell (AML12) and a stable TXNDC5-knockout AML12 [30] cell lines were grown in a humidified atmosphere of 5% CO_2 at 37°C in Dulbecco's modified Eagle's minimum essential medium (DMEM; ThermoFisher Scientific, Waltham, MA, USA): F12-Ham's medium (GE Healthcare Life Science, South Logan, UT) in 1:1 ratio supplemented with 10% fetal bovine serum (ThermoFisher Scientific), 1:500 insulin/transferrin/selenium (Corning, Bedford, MA, USA), 40 ng/mL dexamethasone (Sigma-Aldrich; Merck Millipore, Darmstadt, Germany) 1% nonessential amino acids (ThermoFisher Scientific), 1% amphotericin B (1000 mg/mL; Thermo Fisher Scientific, Waltham, MA, USA),1% penicillin (1000 U/ml; ThermoFisher Scientific), and 1% streptomycin (1,000 mg/mL; ThermoFisher Scientific) in 25-cm^2 flasks (four replicates) for squalene extraction and in six-well plates to RNA isolation (six replicates). Medium was changed every 2 days. When cells reached 90–100% confluency, the medium was removed, and cells were washed twice with phosphate buffered saline (PBS) prior to the addition of the serum-free median without amphotericin B containing 30 μM of squalene loaded in poly(lactic-co-glycolic acid) (PLGA) nanoparticles [30] and incubated for 72 h. In squalene epoxidase inhibitor experiments, cells were treated with 1 μM NB-598 or vehicle for 24 h. Then, media were removed, washed three times with PBS and harvested with trypsin, and the cell pellet was measured prior to squalene

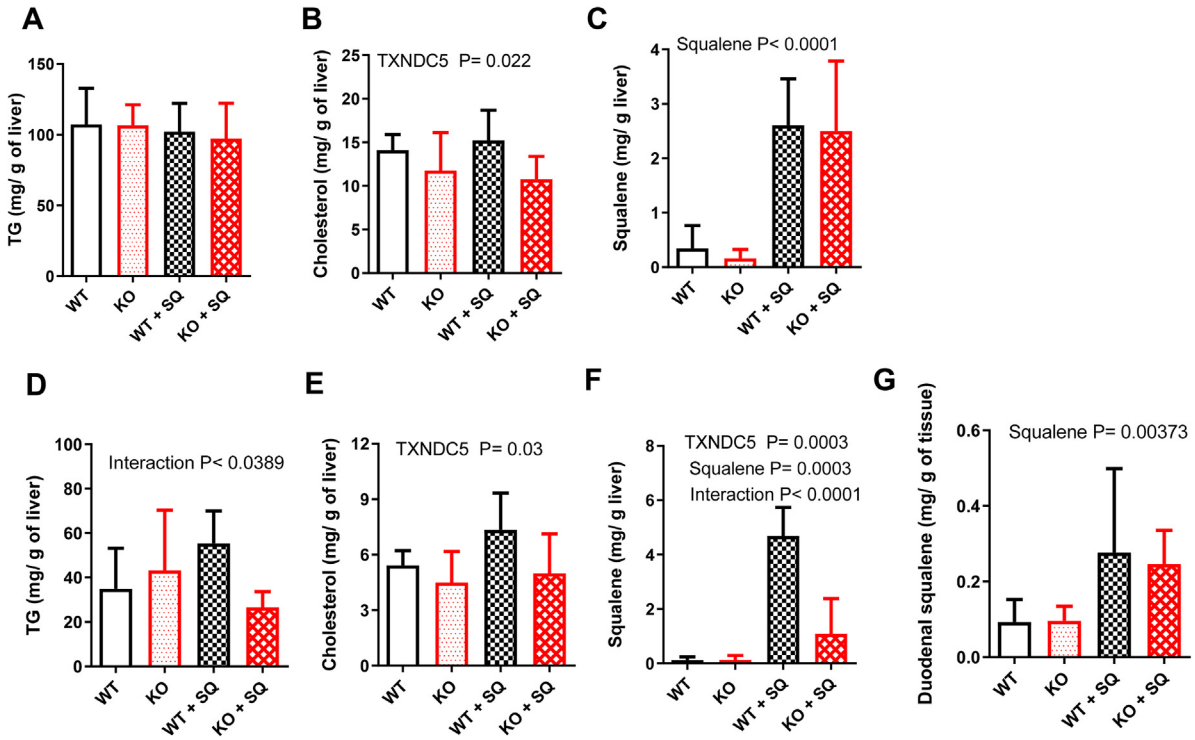

Fig. 1. Lipid parameters in experimental conditions according to sex. The upper panels correspond to females and the lower panels to males. (A and D) hepatic triglyceride; (B and E) hepatic cholesterol; (C and F) hepatic squalene and (G) duodenal squalene content. Results are presented as mean ± SD of six or seven mice. Statistical analyses were done by two-way ANOVA. TXNDC5 indicates the effect of TXNDC5 deficiency; squalene, the effect of its administration; and interaction, the combined effect of both.

extraction. To RNA extraction, media were removed and cells collected with Tri-reagent solution (Ambion), RNA isolation and cDNA synthesis were performed as above described. For microscopy and flow cytometry, median were removed and cells were fixed and stained with Nile Red and Hoechst 33342 as described [30]. Flow cytometry was carried out in a Beckman Coulter Gallios flow cytometer (Brea, CA, USA).

2.12. Statistics

Results are presented as means and their standard deviations. Data distribution was analyzed according to Shapiro–Wilk test, and homology of variance among groups using Bartlett's or Levene's tests. Parameters fitting both hypotheses were analyzed using one-Way ANOVA and Tukeyś test as *post-hoc* comparisons. Nonparametric Mann-Whitney's U test was used to compare the groups failing in any of the hypotheses. Two-way ANOVA was performed using the Sidak test with GraphPad Prism 8 for Windows (GraphPad, S. Diego, CA, USA). Association between variables was assessed by Spearman's correlation coefficient (ρ) using IBM SPSS version 25 software (IBM, Armonk, NY, USA). A P value of less than .05 was considered statistically significant.

3. Results

3.1. Somatometric and histological analyses

In both sexes during the length of dietary intervention, the four experimental groups showed similar body weight gains (Supplementary Fig. 2A and 2E). No statistically significant differences in the ratio of body weight gain/feed intake were observed in females (Supplementary Fig. 2B), but in mice given squalene, the deficiency of TXNDC5 led to lower body weight gain/feed intake (Supplementary Fig. 2F). In female mice, the amount of body weight lost during fasting prior to sacrifice (Supplementary Fig. 2C) showed no significant difference among the studied groups. Nonetheless, male mice lacking TXNDC5 and consuming squalene exhibited a higher reduction in body weight compared to wild-type mice with squalene as well as TXNDC5-KO mice (Supplementary Fig. 2G). This outcome implies a conceivable impact of squalene in the absence of TXNDC5. Finally, the mass of the liver (Supplementary Fig. 2D and 2H) was similar in all the experimental groups in both sexes.

Male *Txndc5*-ko mice accumulated triglycerides and cholesterol in the liver when fed a low-fat diet without changes in lipid droplet area [24]. This report investigates how squalene affects mice with or without TXNDC5, on a C57BL/6J genetic background, when incorporated into a Western diet. In female mice, the hepatic triglyceride levels (Fig. 1A) did not exhibit significant variation in the experimental groups, whereas the absence of TXNDC5 had a negative impact on the hepatic cholesterol levels (Fig. 1B), regardless of the squalene supplementation. However, the hepatic squalene content was enhanced in the female groups that were fed with a squalene-enriched diet (Fig. 1C), and it did not differ upon the absence of TXNDC5 protein. Male wild-type mice that received squalene exhibited a trend to elevated hepatic levels of triglycerides, as depicted in Figure 1D. In contrast, TXNDC5 knockout mice did not show this trend, as there was a significant interaction between the absence of TXNDC5 and the administration of squalene. Also in this sex, the lack of TXNDC5 had a negative impact on the levels of hepatic cholesterol (Fig. 1E). When hepatic squalene content was analyzed, it found that WT males experienced a significant increase when consuming the squalene-supplemented diet (Fig. 1F). Interestingly, TXNDC5 deficiency hindered the accumulation of squalene in the liver. To reject any intestinal malabsorption of squalene, duodenal content was analyzed (Fig. 1G). The ab-

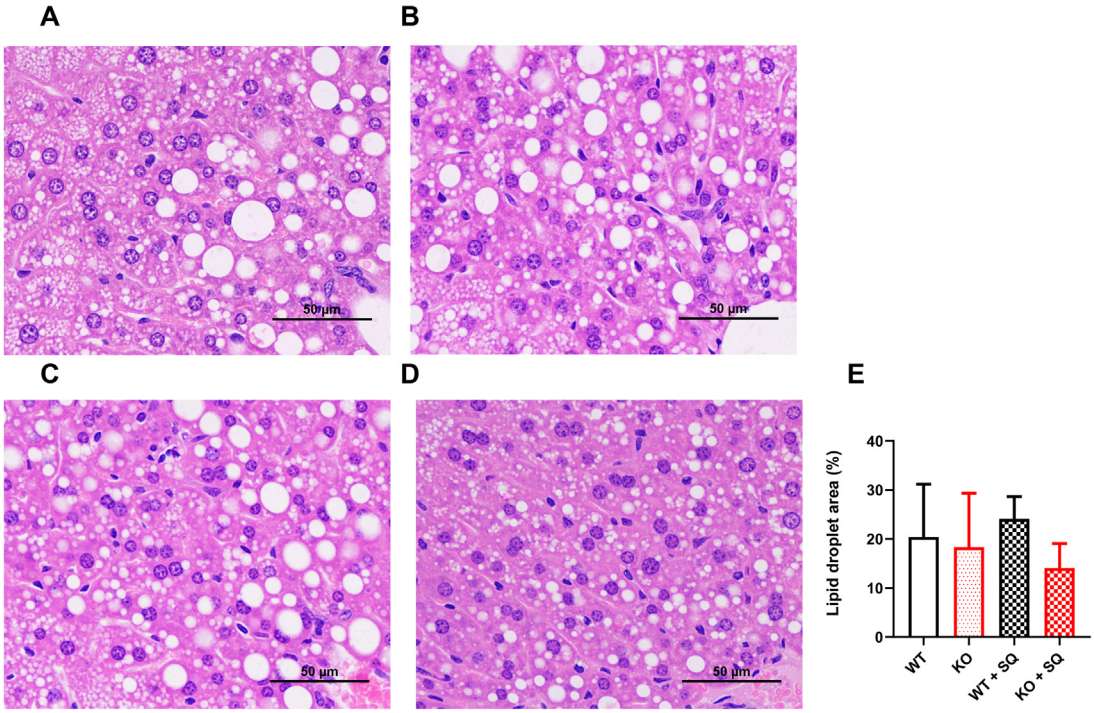

Fig. 2. Hepatic histological analyses in male mice fed with different diets for six weeks. (A) representative liver micrographs from wild-type (WT) mice receiving a purified Western diet; (B) TXNDC5-knock-out (KO) mice fed the Western diet; (C) images from WT mice receiving a purified 1%-squalene (SQ) enriched Western diet and (D) TXNDC5-KO mice fed the purified 1%-squalene enriched Western diet. Liver sections from each animal were stained with hematoxylin and eosin and evaluated blindly. (E) Morphometric difference in the amount of lipid droplet area. Results are shown as mean ± SD of six or seven mice. Statistical analyses were performed by two-way ANOVA.

sence of TXNDC5 did not have a significant impact, as no changes were observed. Overall, there is a sex difference in the influence of TXNDC5 on the accumulation of squalene in the liver. This effect is more prominent in males. Thus, histological analyses were conducted in this group, and representative images of hepatic sections from male mice are presented in Figure 2, panels A to D. A quantitative assessment of lipid droplet areas (Fig. 2E) demonstrated a statistically significant reduction (Mann-Whitney U-test, $P<.01$) in the area occupied by lipid droplets in TXNDC5-KO mice compared to WT mice consuming squalene. These findings align with the reduced hepatic triglyceride content observed. Furthermore, a significant correlation was found between the hepatic lipid droplet area and TG content in this experimental approach ($\rho=0.768$, $p<.001$) (data not shown). In this case, however, the 2-way ANOVA test did not reveal the interaction between TXNDC5 and squalene.

3.2. Isolation and characterization of LDs

Considering our previous results showing that squalene accumulated in lipid droplets [17] and the impact of TXNDC5 deletion on squalene accumulation in males, only hepatic LDs from this sex were prepared and analyzed.

The results of LD-associated proteins obtained by gel-LC-MS/MS were used to generate a profile of their preparations. In Table 1 the abundance of different proteins normalized to that of monoacylglyceride lipase (MGLL) is compiled. According to the displayed results, the amounts of proteins considered to be present into LDs (MGLL, PLIN2, PLIN3, CES1C, CES1D, CES1F, CES3, or RAB7) [23] were similar among the different groups. Golgi and plasma proteins were minimally present, the same occurred for ER, mitochondria, and peroxisomes, although there were important differences depending on the considered marker. For instance, TXNDC5 was found only in wild-type mice receiving squalene and was absent in the rest of the groups. The cytosolic maker (GAPDH) showed an important change between the WT group and the rest of the groups. However, ATPCL was not detected in the prepared LDs.

Using an aliquot of lipid droplet preparations, their lipids were also analyzed in the different groups. As shown in Figure 3A and B, lipid droplets of WT animals receiving squalene showed a trend to increase TG and cholesterol contents. Regarding squalene content (Fig. 3C), the groups administered with the compound displayed elevated values, whereas mice lacking TXNDC5 exhibited significantly lower amounts than the WT+SQ group (significant interaction). The outcomes are consistent with the changes observed in the liver homogenates.

3.3. Hepatic LD-associated proteins in the different experimental conditions

The delipidated lipid droplets purified from the livers were analyzed by gel-LC-MS/MS and the data were refined as described in the materials and methods. According to this analysis, (Supplementary Table 2), 1,326, 1,699, 1,871 and 1,604 proteins were identified in the LDs isolated from WT, KO, WT + SQ and KO + SQ groups, respectively. As shown in Supplementary Figure 3, squalene administration had a profound impact on WT since 643 proteins changed (A) *vs.* squalene administration in KO mice, where only 144 did (B). The absence of TXNDC5 was translated into 482 hits (C) that squalene administration reduced to 85 (D). To reduce the complexity, only identified proteins with three peptides, classified by Mascot as found, with 20% of coverage and a Mascot score higher than 100 were processed (Supplementary Fig. 1). According to these criteria, there were 297 proteins to be compared among the different conditions. Further refinement by selecting those with a $\log_2$ NSAF ratio between groups <-1 or >1 revealed that squalene administration changed 52 proteins in the WT. In the ab-

Table 1
Characteristics of purified hepatic lipid droplets in the different conditions.

	WT	KO	WT+SQ	KO+SQ
Lipid droplets				
MGLL	1.0	1.0	1.0	1.0
PLIN2	0.2	0.7	1.2	0.9
PLIN3	0.05	0.2	0.5	0.2
CES1C	1.2	1.2	1.2	1.6
CES1D	7.3	8.0	9.4	11.2
CES1F	5.9	5.2	5.7	7.6
CES3	0.6	1.0	1.0	0.8
RAB7	2.5	2.0	2.5	2.6
Golgi				
STX7	0.1	0.1	0.1	0.2
GM130	0.0	0.0	0.0	0.0
GOLGA5	0.0	0.0	0.0	0.0
Plasma membrane				
CADH2	0.0	0.1	0.1	0.1
ESYT2	0.02	0.02	0.02	0.03
FLOT1	0.0	0.0	0.0	0.0
Endoplasmic reticulum				
CANX	0.5	0.8	1.3	1.3
GRP78	0.0	0.0	0.0	0.0
HSPA5	1.3	1.9	2.3	2.6
PEMT	0.0	0.0	0.0	0.0
TXNDC5	0.0	0.0	0.2	0.0
VPS13A	0.0	0.0	0.0	0.0
Cytosol				
GAPDH	7.9	18.5	17.9	19.4
ATPCL	0.0	0.0	0.0	0.0
Mitochondria				
COX4I1	0.2	1.6	1.9	1.7
CPT2	1.0	1.2	1.5	1.7
ACSL1	0.8	1.9	2.3	2.2
VDAC	0.7	1.0	1.0	1.4
Peroxisomes				
PEX3	0.0	0.1	0.2	0.0
PMP34	0.0	0.0	0.1	0.0

Results represent the normalized spectral abundance factor (NSAF) of the different proteins normalized to the value of MGLL.

sence of TXNDC5, squalene administration affected the amount of eight proteins (Supplementary Fig. 1). Common proteins responding to squalene administration in WT and TXNDC5-KO resulted in six proteins as shown in the Venn diagram (Supplementary Figure 1B). These are listed in Table 2: cytosolic 10-formyltetrahydrofolate dehydrogenase (ALDH1L1), mitochondrial fumarate hydratase (FH), adenosine kinase (ADK), mitochondrial agmatinase (AGMAT), calreticulin (CALR), and adipocyte plasma membrane-associated protein (APMAP).

The pathway enrichment analysis of the 52 proteins whose expression was changed by squalene administration compared to WT is shown in Figure 4A. They fell into eight major categories: carbon metabolism, cytochrome P450, pathologies, chemical carcinogenesis, oxidative phosphorylation, thermogenesis, arginine biosynthesis, and amino acid metabolism. They were grouped into five networks according to STRING (Fig. 4B). The absence of TXNDC5 (Supplementary Fig. 1) resulted in 44 proteins with altered expression belonging to the categories: carbon metabolism, chemical carcinogenesis, amino acid metabolism, cytochrome P450, and organic and fatty acid metabolism (Fig. 4C). They were grouped into seven networks according to STRING (Fig. 4D).

To confirm the LD association of some of the identified proteins, and their changes in the different conditions, their abundance in LDs and liver homogenates was assessed by immunoblotting. In a previous experiment with *Apoe*-deficient mice fed a chow diet [15], squalene induced increased levels of TXNDC5 and CALR in hepatic microsomal preparations. Under the present conditions in WT animals consuming a Western diet, mice receiving squalene showed a modest increase in the amount of TXNDC5 in the homogenate (Fig. 5A and B), but a significant increase in lipid droplets ($P<.05$ by Mann-Whitney U-test) which was not supported by the two-way ANOVA (Fig. 5C and D). Obviously, TXNDC5-KO mice did not show this protein in either homogenate or lipid droplets. When CALR was assayed in homogenate (Fig. 5E and F), minimal changes were observed in the different experimental conditions. However, squalene administration in WT animals resulted in an increased content of this protein in lipid droplets (Fig. 5G and H), which was abolished in the absence of TXNDC5. When APMAP was assayed, the same pattern was observed, although its decrease in lipid droplets was less pronounced in the absence of TXNDC5 (Fig. 5K and L). Overall, the squalene administration favors the presence TXNDC5, CALR and APMAP in lipid droplets and the lack of TXNDC5 results in a decreased presence of these proteins.

3.4. RNA analyses of squalene administration target genes

In order to support the observed squalene-induced changes, mRNA analyses of some previously characterized target genes [16] were carried out by RT-qPCR. *Txndc5* mRNA levels were not influenced by squalene administration but as expected TXNDC5-KO animals showed a low level of expression. As previously observed [16], squalene administration induced the hepatic expression of *Cyp2b10, Cyp2c55,* and *Cyp3a41* (Fig. 6) and the absence of TXNDC5 did not suppress this effect. A correlation analysis also reinforced the association among these hepatic gene expressions and squalene content (Supplementary Fig. 4). No significant changes were observed for *Acox1, Apmap, Arf5,* and *Calr* (Fig. 6). Taken together, these results suggest that the absence of TXNDC5 does not influence the transcriptional changes induced by squalene administration.

Table 2
Changes in hepatic lipid droplet-associated proteins in the different experimental conditions influenced by squalene administration.

Accession	Description	WT+SQ/ WT	WT+SQ/ KO + SQ	KO+SQ/ KO
Q8R0Y6	Cytosolic 10-formyltetrahydrofolate dehydrogenase (ALDH1L1)	1.0	1.4	-1.3
P97807	Mitochondrial fumarate hydratase (FH)	1.0	1.3	-1.1
P55264	Adenosine kinase (ADK)	1.7	1.1	-0.5
A2AS89	Mitochondrial agmatinase (AGMAT)	1.6	1.1	-0.7
P14211	Calreticulin (CALR)	1.6	1.0	-0.5
Q9D7N9	Adipocyte plasma membrane-associated protein (APMAP)	2.1	1.0	0.2

Results represent the $\log_2$ of ratio of normalized spectral abundance factors of the specified conditions (NSAF).

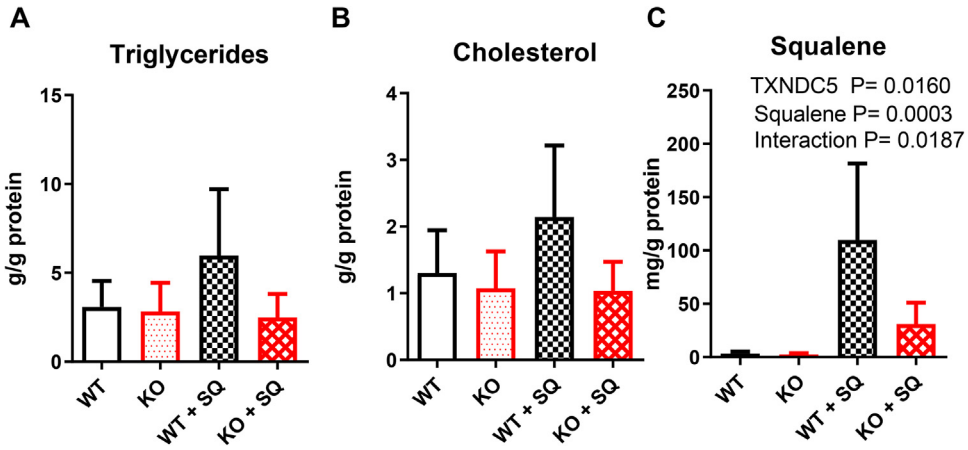

Fig. 3. Lipid composition of male hepatic lipid droplets. (A) triglycerides; (B) cholesterol and (C) squalene content. Results are expressed as mean ± SD of six or seven mice. Two-way ANOVA was used for statistical analysis. TXNDC5 indicates the effect of TXNDC5 deficiency; squalene, the effect of its administration; and interaction, the combined effect of both.

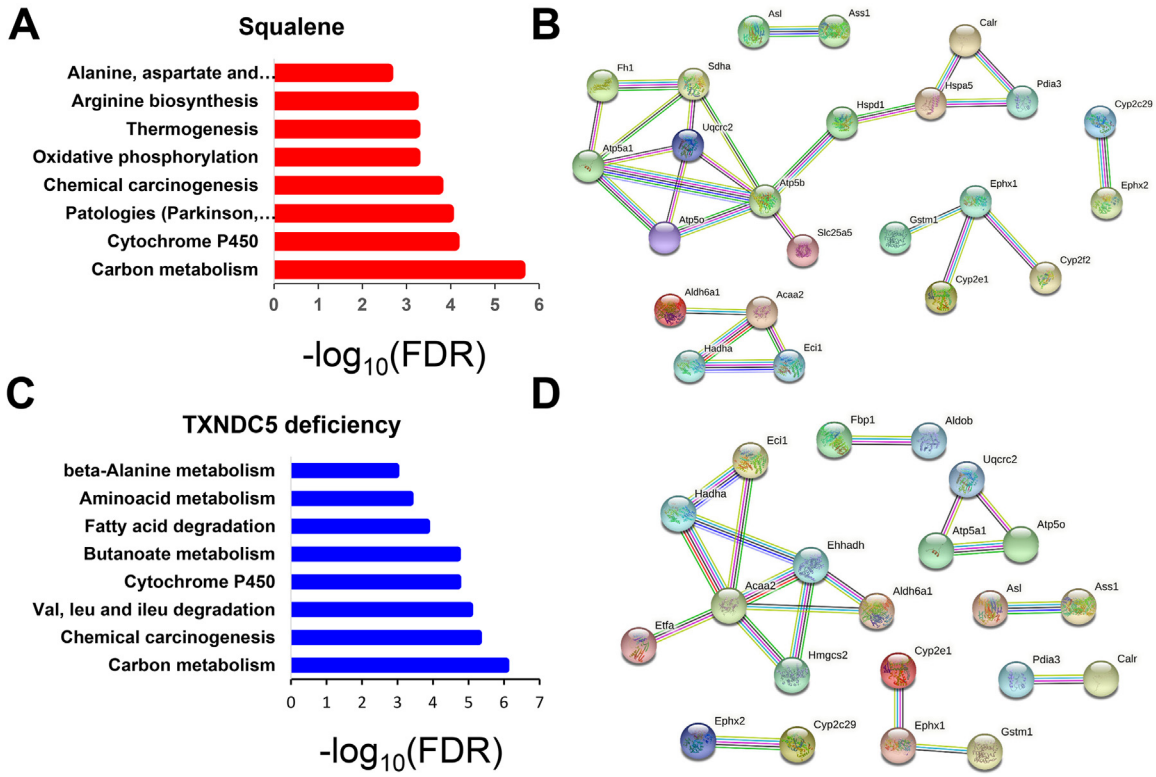

Fig. 4. Hepatic lipid droplet-associated proteins found to be significantly changed by the influence of squalene or TXNDC5 deficiency in mice. (A) Pathway enrichment of differentially expressed proteins in squalene-supplemented animals expressed as the -$\log_{10}$ (FDR) according to KEGG. (B) STRING (https://string-db.org/) network of top differentially expressed proteins by the influence of squalene with a confidence level of 0.9. (C) Pathway enrichment of differentially lipid droplet-associated proteins in TXNDC5 deficiency expressed as the -$\log_{10}$ (FDR) according to KEGG. (D) STRING network of top differentially expressed proteins in TXNDC5 deficiency with a confidence level of 0.9.

3.5. Analyses in WT and TXNDC5-KO AML12 cell lines

To verify whether the observed changes in response to squalene could be reproduced in a hepatic cell line, WT and TXNDC5-KO AML12 cell lines were used and incubated in the presence of polymeric biodegradable nanoparticles loaded with squalene. Squalene-loaded PLGA nanoparticles were used to favor squalene aqueous availability and cellular uptake compared to the administration of the free isoprenoid [30]. As shown in Figure 7 (panels A–E), squalene incubation resulted in an increased cellular squalene content, which was significantly reduced in the absence of TXNDC5. This result was confirmed by flow cytometry of squalene-loaded cells (Fig. 7F). When cell squalene was monitored at different time points, TXNDC5-KO cells accumulated less of this compound (Fig. 7G), which was released into the medium (Fig. 7H). Squalene accumulation in the presence of a squalene epoxidase inhibitor was also lower in TXNDC5-KO AML12 cells compared to WT-AML12 (Fig. 7I). Thus, the mouse findings were reproduced *in vitro*. Gene expression was also examined. Surprisingly, *Cyp2b10* expression was decreased by squalene incubation and this effect was more pronounced in the absence of TXNDC5 (Fig. 7J). *Cyp2c55* and *Cyp3a41* expressions were increased by squalene incubation

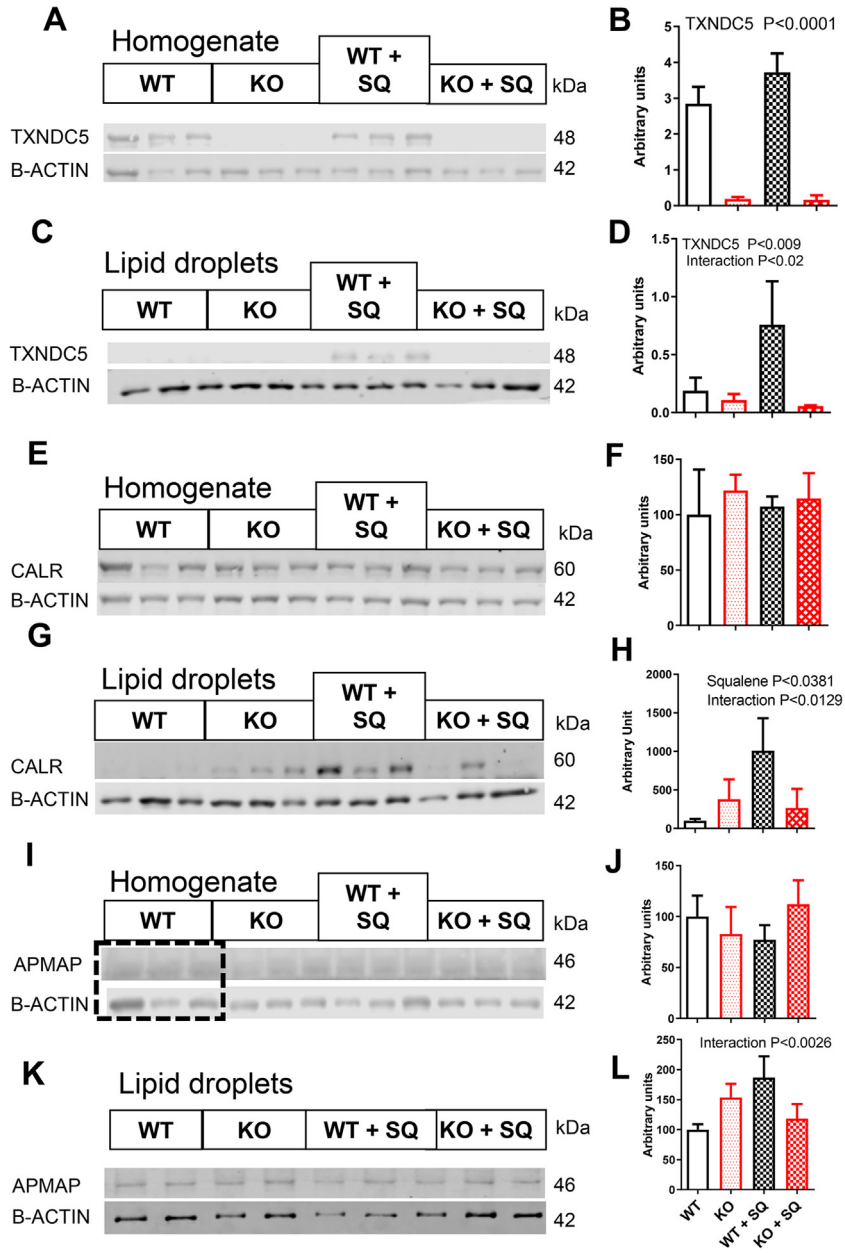

Fig. 5. Hepatic protein expressions. (A) Representative Western images of liver homogenates. (B) Quantitative results of TXNDC5 normalized to β-ACTIN. (C) Representative Western images of lipid droplets. (D) Quantitative results of TXNDC5 normalized to β-ACTIN. (E) Representative Western images of liver homogenates. (F) Quantitative results of CALR normalized to β-ACTIN. (G) Representative Western images of lipid droplets. (H) Quantitative results of CALR normalized to β-ACTIN. (I) Representative Western images of liver homogenates. The left three samples included in dashed rectangle correspond to two non-adjacent parts of the same gel. (J) Quantitative results of APMAP normalized to β-ACTIN. (K) Representative Western images of lipid droplets. (L) Quantitative results of APMAP normalized to β-ACTIN. Results are shown as mean ± SD. Statistical analyses were performed by two-way ANOVA. TXNDC5 indicates the effect of TXNDC5 deficiency, squalene, the effect of its administration and interaction, the combined effect of both.

(Fig. 7K and L). TXNDC5 deletion partially abolished the squalene effect on *Cyp2c55* ($P<.05$ by Mann-Whitney U-test), which was not supported by the two-way ANOVA, and had no effect on *Cyp3a41* expression.

4. Discussion

The aim of the present study was to verify the influence of TXNDC5 on the hepatic management of squalene provided in a Western diet. Our results indicate that mice consuming a 1% squalene-supplemented Western diet (corresponding to a dose of 1 g/kg body weight) showed a sexual dimorphism in the sense that the absence of TXNDC5 blocked hepatic squalene accumulation in a tissue-specific manner only in males. When hepatic lipid droplets were isolated and characterized, TXNDC5 accumulated in this subcellular compartment in hydrocarbon-fed mice and as expected, was absent in TXNDC5 KO mice. The latter mice were unable to store squalene in lipid droplets according to the pattern observed in the whole liver. A highly stringent protein selection scheme to detect those involved in the squalene response under all conditions led to the identification of ALDH1L1, FH, ADK, AGMAT, CALR, and APMAP. Independent confirmation showed that CALR and APMAP accumulated in lipid droplets in the presence of squalene and that this fact was influenced by TXNDC5. To support the specificity of

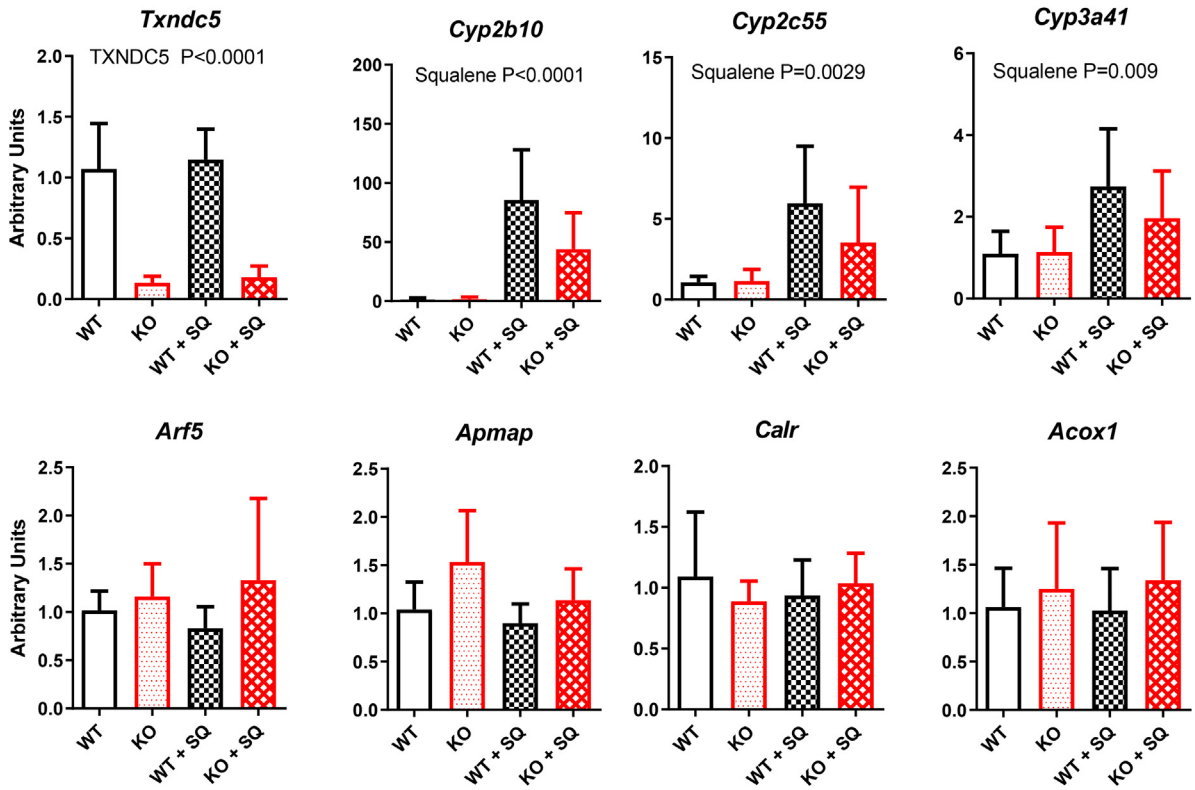

Fig. 6. Hepatic mRNA expression of selected genes in males. Results are shown as means ± SD of six or seven mice. Statistical analyses were performed by two-way ANOVA. TXNDC5 indicates the effect of TXNDC5 deficiency and squalene, the effect of its administration.

this finding, hepatic expression of previously characterized squalene gene targets was analyzed, and squalene administration induced hepatic expression of *Cyp2b10, Cyp2c55,* and *Cyp3a41* and the absence of TXNDC5 did not suppress this effect. The increase in squalene content was reproduced *in vitro* using squalene delivered as nanoparticles to an AML12 liver cell line. A phenomenon that was stopped in an engineered cell line lacking TXNDC5. In this model, *Cyp2c55* and *Cyp3a41* expression was increased by squalene, and TXNDC5 deletion partially abolished the effect of squalene on *Cyp2c55* and had no effect on *Cyp3a41* expression. Collectively, squalene accumulation in lipid droplets is sex dependent on TXNDC5, but its downstream effects on gene expression appear to be independent of this protein.

The observed sexual dimorphism in squalene response is something that confirms our previous findings in *Apoe*-deficient mice, where the reduction of atherosclerotic lesions was associated with hepatic fat content only in males [12]. In the search of proteins involved in these lipid changes, male microsomal TXNDC5 protein was found to be increased by squalene administration and significantly associated with hepatic fat content [15]. To establish the molecular mechanisms associating this protein with squalene intake, TXNDC5-KO mice of both sexes were generated [24] and fed a Western diet with or without squalene. When their livers were analyzed for squalene content, the absence of TXNDC5 abolished the hepatic squalene accumulation only in males. This phenomenon did not occur in the duodenum either, rejecting the hypothesis of an intestinal malabsorption of squalene and suggesting that represents a sex- and tissue-specific mechanism. To further characterize this observation and to benefit from a previous finding that squalene accumulated in lipid droplets of male mice [17], the latter were the focus of attention.

Shotgun proteomics via LC-MS/MS was used to characterize the mouse hepatic LD proteome in the different experimental conditions. The identified associated proteins ranged from 1,326 to 1,871 (Supplementary Table 1), which is consistent with reports of 1,520 using a high-fat diet [31], 932 [32], or 810 [23], 613 [33] in the fasting state. More recently, 4,515 unique proteins were found in mice consuming a high-fat diet (60% of calories as fat content for 18 weeks) [34]. An important concern when analyzing organelle proteomes is the purity of the preparations. As expected, the canonical LD-marker proteins PLIN2 and PLIN3 were present in our LD preparations (Table 1). Likewise, MGLL was a component of the prepared lipid droplets. In fact, the latter was found to be extraordinarily consistent among the different lipid preparations, so it was used as a reference protein to normalize the abundance of other proteins. Although PLIN2 has been used as a normalization protein [23], other authors have raised concerns about its suitability as a LD marker since it is not present on all hepatic LDs [31]. Furthermore, PLIN2 has been found to increase in 24-four fasting and decrease after refeeding [23]. Using, an extreme fat content (60% of calories) for 9 weeks [31] or the same high-fat diet for refeeding [35], this protein was found particularly abundant. In the present report, due to the short duration of the Western diet (6 weeks), the relatively low percentage of fat (35% of calories) and a 16-h fasting period, PLIN2 was not particularly abundant and variable among the different experimental conditions. Interestingly, DGAT2, CIDEA, CIDEB, CIDEC, ATGL (PNPLA2) were not found in our lipid droplets and CGI-58 (ABHD5) was present only under certain conditions. In contrast, others such as RAB7 [34] was consistently present. Using a fat content (60% of calories) for 12 weeks, Krahmer et al. [36] reported that the plasma membrane-ER contact site protein ESYT2 was increased in their LD preparations. In our case, lipid droplets were poorly enriched in this protein. Mitochondrial

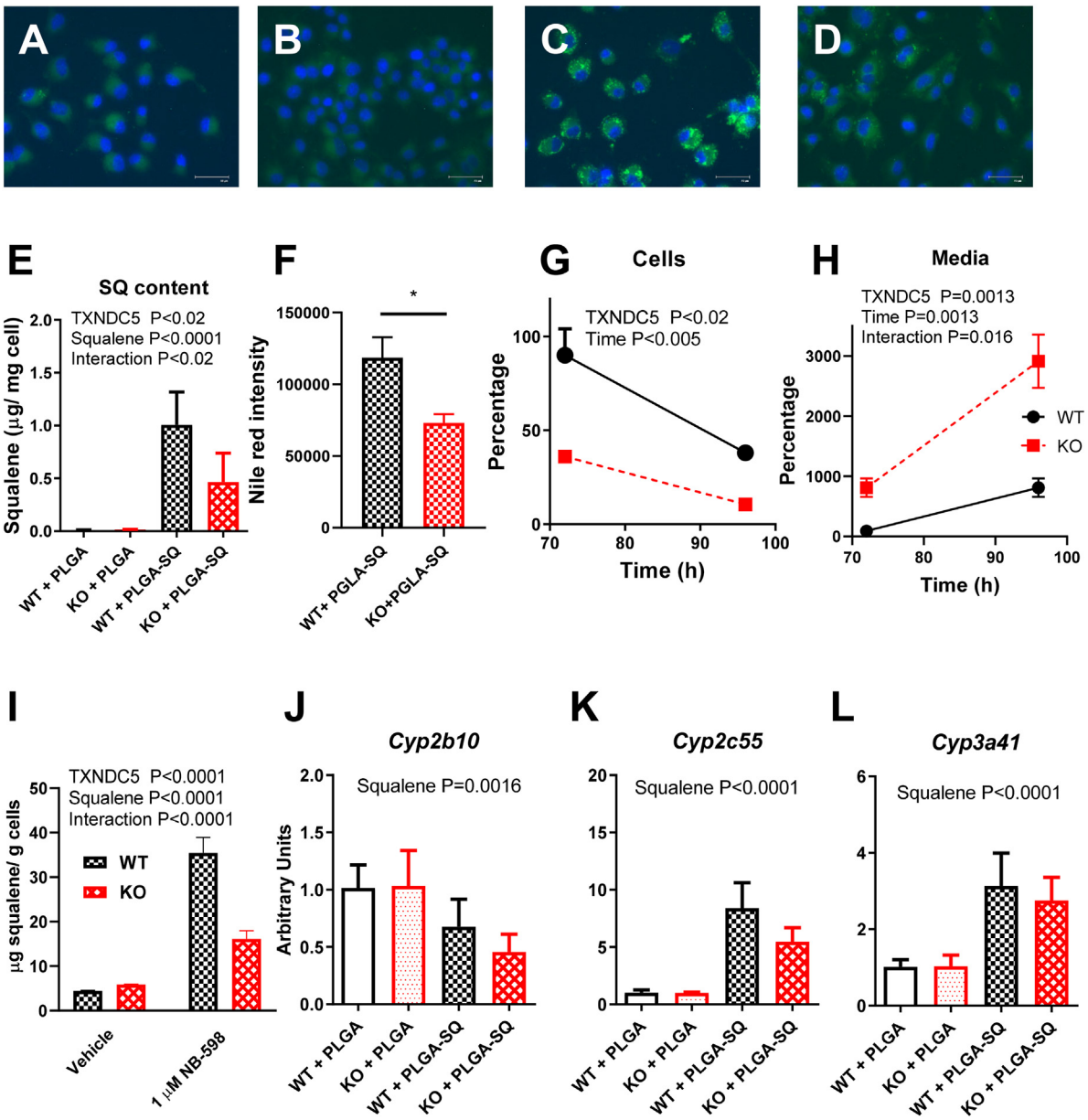

Fig. 7. Influence of TXNDC5 on squalene incubation of AML12. Nile red and Hoechst fluorescence staining of cultured cells. (A) WT+ PGLA; (B) KO+ PGLA; (C) WT+ PGLA + SQ and (D) KO+ PGLA + SQ. (E) Squalene content; (F) flow cytometry analyses of Nile red stained lipid droplets. Follow-up of cell (G) and medium (H) squalene content at different time points. Results are expressed as means and SD. In these experiments, cells were incubated for 72 hours in the presence of PGLA-squalene, then this medium was removed, and cells washed and analysed at this time-point and 24 h after incubation in a medium deprived of PGLA-squalene. (I) Squalene content with and without squalene epoxidase inhibition. *Cyp2b10* (J), *Cyp2c55* (K) and *Cyp3a41* (L) mRNA expressions. Results are expressed as mean ± SD of three preparations in duplicate. Statistical analysis was conducted using a two-way ANOVA. TXNDC5 demonstrates the impact of its deficiency, while squalene reveals the effects of its administration. The combined effect of both is seen through their interaction.

markers ACSL1, COX4I1, CPT2, VDAC [35] were present, while peroxisomal and Golgi markers were almost absent. Surprisingly, a cytosolic marker GAPDH was increased, whereas ATPCL [31] was not detected. Regarding ER-localized proteins, a particular profile was also observed, while CES3 or CANX were found, in agreement with Kramer et al. [23], PEMT or GRP78 [35] were absent in our LD preparation, so was VPS13A, proposed by Krahmer et al. [36] as ER protein capable of contacting with mitochondria. Another ER protein, TXNDC5, also previously found in lipid droplets [23], accumulated in this subcellular compartment in the hydrocarbon-fed mice and as expected, was absent in TXNDC5-KO mice. Lipid droplet-associated proteins have been proposed as the drivers to achieve their metabolic functions [36]. While the extent of dietary intervention has been shown to modulate the number of LD-associated proteins [36] as well as the duration of fasting [23], little attention has been paid to the amount of fat provided [35] and even less to the composition of those dietary fats or oils. In light of the present findings, where a single fatty compound, squalene, has a profound impact, a new avenue is emerging.

The male TXNDC5-KO mice were unable to store squalene in lipid droplets following the pattern observed in the whole liver, which was reproduced *in vitro* using squalene delivered as nanoparticles to AML12-WT and AML12-TXNDC5-KO hepatic cell lines, observing a lower amount of squalene in the absence of TXNDC5. This would suggest that hepatocytes are the main cells involved in this squalene storage. Furthermore, using a squa-

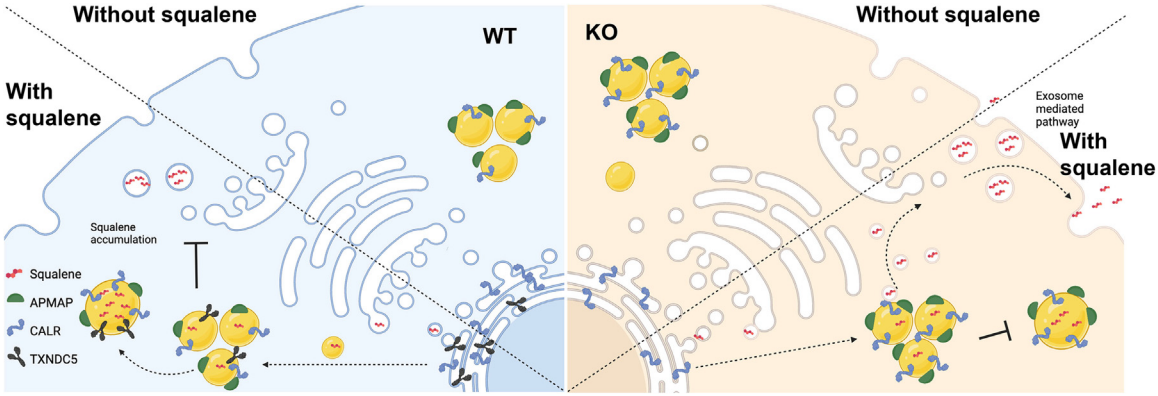

Fig. 8. Summary of the proposed mechanism in the absence of TXNDC5 in the accumulation or secretion of squalene. Wild-type (WT) mice receiving a purified Western diet (without squalene) and WT mice receiving a purified 1%-squalene enriched Western diet (with squalene). TXNDC5-knock-out (KO) mice fed the Western diet (without squalene) and TXNDC5-KO mice fed the purified 1%-squalene enriched Western diet (with squalene).

lene epoxidase inhibitor without squalene administration, a higher amount of squalene was also observed in AML12-WT and this process was impaired in the absence of TXNDC5. To gain more insight into the altered mechanisms of squalene accumulation or favored secretion in this experimental setting, a proteomic approach of lipid droplets was performed. A highly stringent protein selection scheme to detect those responding to the squalene administration under all conditions led to the identification of ALDH1L1, FH, ADK, AGMAT, CALR, and APMAP. Independent confirmation by Western blot analysis showed that CALR and APMAP were associated with lipid droplets in the presence of squalene and this fact was influenced by TXNDC5. The change in CALR was neither transcriptional nor translational, as its hepatic mRNA and protein levels were not altered. CALR was involved in preventing the secretion of Z-antitrypsin (ZAAT) in a complex with ERdj3 through an exosome-mediated pathway [37]. When ERdj3 was depleted [38], the rate of ZAAT degradation in hepatocytes increased by redirecting ZAAT proteasome-dependent degradation through autophagosome formation. Our lipid droplets were depleted of ERdj3, but although they contained antitrypsin, this was not enriched by squalene administration. Squalene seems to modulate the presence of CALR in lipid droplets only in the presence of TXNDC5, favoring its accumulation. A hypothetical situation would be that incorrect CALR modulation in the absence of TXNDC5 promotes squalene secretion through an exosome-mediated pathway. Adipocyte plasma membrane associated protein (APMAP, also known as C20orf3) has been proposed as a plasma membrane and endoplasmic reticulum protein with hydrolase activity. Originally discovered in adipocytes, it has also been described in the liver [39,40]. The observed changes in APMAP are related to its lipid droplet association, since no change was observed in liver homogenate, nor in mRNA levels. The reduced accumulation of squalene in the whole liver of TXNDC5-KO mice would favor an exosome-mediated pathway of secretion of this compound, and the role of APMAP as a membrane linker would contribute to this (Fig. 8). These findings suggest a central role for TXNDC5 in maintaining squalene in lipid droplets in hepatocytes. Experiments in yeast have shown that the accumulation of squalene in lipid droplets avoids undesirable effects of this compound such as growth defects and loss of viability [41]. In addition, squalene storage increases with LD volume expansion and is easily deformed to move through intertwined chains of triacylglycerols in the LD core [42]. Furthermore, the sequestering of squalene in lipid droplets would limit the activation of squalene monooxygenase and cholesterol biosynthesis [43]. In a model of steatohepatitis, squalene supplementation decreased some hepatic triglyceride species (TG[54:2], TG[55:0], and TG[55:2]) [44]. In light of these findings, squalene plays an important role on lipid droplets and these are involved in limiting its action. The present findings indicate that squalene requires TXNDC5 to be retained in LD. Otherwise, it is lost via a putative exosomal pathway. However, inactivation of TXNDC5 has been found to reduce liver fibrosis [45]. Further experimental support is needed to reconcile these findings and the suggestive hypotheses emerging from this work.

Hepatic expressions of previously characterized squalene gene targets (*Cyp2b10, Cyp2c55,* or *Cyp3a41*) [16] were analyzed to investigate whether or not the response was modified by the absence of TXNDC5 either *in vivo* or *in vitro*. While both models reproduced the induction of *Cyp2c55* and *Cyp3a41* by squalene administration, the changes in *Cyp2b10* were different between the *in vivo* and the *in vitro* approaches. Equally different was the relevance of the TXNDC5 absence, while maintaining a tendency it hardly modified the squalene effect, *in vivo* or *in vitro*, respectively. These gene changes are consistent with the data that some changes in gene expression in squalene action are carried out independently of its accumulation in lipid droplets, which is in agreement with the early work of Tilvis et al. who proposed two pools of squalene in adipocytes [46].

In conclusion, squalene accumulation in lipid droplets is sex dependent on TXNDC5, but its downstream effects on gene expression are independent of this protein. The lack of hepatic squalene accumulation in LD in the absence of TXNDC5 would be possible through an exosome-mediated pathway involving CALR and APMAP. Our results also highlight the importance of a single dietary component, squalene, on the dynamics of LD-associated proteins and the role of TXNDC5 in controlling specific lipid droplets.

Declaration of competing interest

The authors declare no conflict of interest and the funders had no role in the design of the study; in the collection, analyses, or interpretation of data; in the writing of the manuscript, or in the decision to publish the results.

Acknowledgments

We thank Jose Luis Pitarch, Cristian Alvarez, Silvia Garcés and Mª Pilar Lierta for their help in maintaining the animals.

Declaration of generative AI and AI-assisted technologies in the writing process

During the preparation of this work, the authors used DeepL Write (DeepL SE, Cologne, Germany) in order to improve English use. After using this tool, the authors reviewed and edited the content as needed and take(s) full responsibility for the content of the publication.

Funding

This research was supported by grants (CIBEROBN, CB06/03/1012) from CIBER Fisiopatología de la Obesidad y Nutrición as an initiative of FEDER-ISCIII, Ministerio de Ciencia e Innovación-Fondo Europeo de Desarrollo Regional (PID2019-104915RB-I00 and PID2022-104915RB-I00) and Fondo Social Europeo-Gobierno de Aragón (B16_23R). S.H.B. was recipient of a joint fellowship from the Universities of Zaragoza and Pau and J.S.-M. was recipient of a Fundación Cuenca Villoro fellowship.

Supplementary materials

Supplementary material associated with this article can be found, in the online version, at doi:10.1016/j.jnutbio.2023.109503.

References

[1] Guasch-Ferré M, Willett WC. The Mediterranean diet and health: a comprehensive overview. J Intern Med 2021;290:549–66.
[2] Shannon OM, Ashor AW, Scialo F, Saretzki G, Martin-Ruiz C, Lara J, et al. Mediterranean diet and the hallmarks of ageing. Eur J Clin Nutr 2021;75:1176–92.
[3] Gaforio JJ, Visioli F, Alarcon-de-la-Lastra C, Castaner O, Delgado-Rodriguez M, Fito M, et al. Virgin olive oil and health: summary of the iii international conference on virgin olive oil and health consensus report, JAEN (Spain) 2018. Nutrients 2019;11:2039.
[4] Guasch-Ferré M, Li Y, Willett WC, Sun Q, Sampson L, Salas-Salvadó J, et al. Consumption of olive oil and risk of total and cause-specific mortality among U.S. adults. J Am Coll Cardiol 2022;79:101–12.
[5] Covas MI, Ruiz-Gutiérrez V, de la Torre R, Kafatos A, Lamuela-Raventós RM, Osada J, et al. Minor components of olive oil: evidence to date of health benefits in humans. Nutr Rev 2006;64:s20–30.
[6] Lou-Bonafonte JM, Arnal C, Navarro MA, Osada J. Efficacy of bioactive compounds from extra virgin olive oil to modulate atherosclerosis development. Mol Nutr Food Res 2012;56:1043–57.
[7] Lou-Bonafonte JM, Fito M, Covas MI, Farras M, Osada J. HDL-related mechanisms of olive oil protection in cardiovascular disease. Curr Vasc Pharmacol 2012;10:392–409.
[8] Lou-Bonafonte JM, Martinez-Beamonte R, Sanclemente T, Surra JC, Herrera–Marcos LV, Sanchez-Marco J, et al. Current insights into the biological action of squalene. Mol Nutr Food Res 2018:e1800136.
[9] Martinez-Beamonte R, Sanclemente T, Surra JC, Osada J. Could squalene be an added value to use olive by-products? J Sci Food Agric 2020;100:915–25.
[10] Gaforio JJ, Sánchez-Quesada C, López-Biedma A, Ramírez-Tortosa MC, Warleta F. Molecular aspects of squalene and implications for olive oil and the mediterranean diet. In: Preedy VR, Watson RR, editors. The mediterranean diet. Amsterdam, The Netherlands: Elsevier; 2015. p. 281–90.
[11] Lovaszi M, Mattii M, Eyerich K, Gacsi A, Csanyi E, Kovacs D, et al. Sebum lipids influence macrophage polarization and activation. Br J Dermatol 2017;177:1671–82.
[12] Guillen N, Acin S, Navarro MA, Perona JS, Arbones-Mainar JM, Arnal C, et al. Squalene in a sex-dependent manner modulates atherosclerotic lesion which correlates with hepatic fat content in apoE-knockout male mice. Atherosclerosis 2008;197:72–83.
[13] Sánchez-Quesada C, Gutiérrez-Santiago F, Rodríguez-García C, Gaforio JJ. Synergistic effect of squalene and hydroxytyrosol on highly invasive MDA-MB-231 breast cancer cells. Nutrients 2022;14:255.
[14] Ramirez-Torres A, Barcelo-Batllori S, Fernandez-Vizarra E, Navarro MA, Arnal C, Guillen N, et al. Proteomics and gene expression analyses of mitochondria from squalene-treated apoE-deficient mice identify short-chain specific acyl–CoA dehydrogenase changes associated with fatty liver amelioration. J Proteomics 2012;75:2563–75.
[15] Ramirez-Torres A, Barcelo-Batllori S, Martinez-Beamonte R, Navarro MA, Surra JC, Arnal C, et al. Proteomics and gene expression analyses of squalene–supplemented mice identify microsomal thioredoxin domain-containing protein 5 changes associated with hepatic steatosis. J Proteomics 2012;77:27–39.
[16] Gabas-Rivera C, Jurado-Ruiz E, Sanchez-Ortiz A, Romanos E, Martinez-Beamonte R, Navarro MA, et al. Dietary squalene induces cytochromes Cyp2b10 and Cyp2c55 independently of sex, dose, and diet in several mouse models. Mol Nutr Food Res 2020;64:e2000354.
[17] Martinez-Beamonte R, Alda O, Sanclemente T, Felices MJ, Escusol S, Arnal C, et al. Hepatic subcellular distribution of squalene changes according to the experimental setting. J Physiol Biochem 2018;74:531–8.
[18] Gluchowski NL, Becuwe M, Walther TC, Farese RV Jr. Lipid droplets and liver disease: from basic biology to clinical implications. Nat Rev Gastroenterol Hepatol 2017;14:343–55.
[19] Olzmann JA, Carvalho P. Dynamics and functions of lipid droplets. Nat Rev Mol Cell Biol 2019;20:137–55.
[20] Loomba R, Friedman SL, Shulman GI. Mechanisms and disease consequences of nonalcoholic fatty liver disease. Cell 2021;184:2537–64.
[21] Scorletti E, Carr RM. A new perspective on NAFLD: Focusing on lipid droplets. J Hepatol 2022;76:934–45.
[22] Horna-Terrón E, Pradilla-Dieste A, Sánchez-de-Diego C, Osada J. TXNDC5, a newly discovered disulfide isomerase with a key role in cell physiology and pathology. Int J Mol Sci 2014;15:23501–18.
[23] Kramer DA, Quiroga AD, Lian J, Fahlman RP, Lehner R. Fasting and refeeding induces changes in the mouse hepatic lipid droplet proteome. J Proteomics 2018;181:213–24.
[24] Sánchez-Marco J, Martínez-Beamonte R, Diego AD, Herrero-Continente T, Barranquero C, Arnal C, et al. Thioredoxin domain containing 5 suppression elicits serum amyloid A-containing high-density lipoproteins. Biomedicines 2022;10:709.
[25] Reeves PG, Rossow KL, Lindlauf J. Development and testing of the AIN-93 purified diets for rodents: results on growth, kidney calcification and bone mineralization in rats and mice. J Nutr 1993;123:1923–31.
[26] Ontko JA, Perrin LW, Horne LS. Isolation of hepatocellular lipid droplets: the separation of distinct subpopulations. J Lipid Res 1986;27:1097–103.
[27] McIlwain S, Mathews M, Bereman MS, Rubel EW, MacCoss MJ, Noble WS. Estimating relative abundances of proteins from shotgun proteomics data. BMC Bioinf 2012;13:308.
[28] Herrera-Marcos LV, Martínez-Beamonte R, Macías-Herranz M, Arnal C, Barranquero C, Puente-Lanzarote JJ, et al. Hepatic galectin-3 is associated with lipid droplet area in non-alcoholic steatohepatitis in a new swine model. Sci Rep 2022;12:1024.
[29] Herrera-Marcos LV, Sancho-Knapik S, Gabas-Rivera C, Barranquero C, Gascon S, Romanos E, et al. Pgc1a is responsible for the sex differences in hepatic Cidec/Fsp27beta mRNA expression in hepatic steatosis of mice fed a Western diet. Am J Physiol Endocrinol Metab 2020;318:E249–EE61.
[30] Bidooki SH, Alejo T, Sánchez-Marco J, Martínez-Beamonte R, Abuobeid R, Burillo JC, et al. Squalene loaded nanoparticles effectively protect hepatic AML12 cell lines against oxidative and endoplasmic reticulum stress in a TXNDC5-dependent way. Antioxidants 2022;11:581.
[31] Khan SA, Wollaston-Hayden EE, Markowski TW, Higgins L, Mashek DG. Quantitative analysis of the murine lipid droplet-associated proteome during diet-induced hepatic steatosis. J Lipid Res 2015;56:2260–72.
[32] Liu M, Ge R, Liu W, Liu Q, Xia X, Lai M, et al. Differential proteomics profiling identifies LDPs and biological functions in high-fat diet-induced fatty livers. J Lipid Res 2017;58:681–94.
[33] Baumeier C, Kaiser D, Heeren J, Scheja L, John C, Weise C, et al. Caloric restriction and intermittent fasting alter hepatic lipid droplet proteome and diacylglycerol species and prevent diabetes in NZO mice. Biochim Biophys Acta 2015;1851:566–76.
[34] Nerstedt A, Kurhe Y, Cansby E, Caputo M, Gao L, Vorontsov E, et al. Lipid droplet-associated kinase STK25 regulates peroxisomal activity and metabolic stress response in steatotic liver. J Lipid Res 2020;61:178–91.
[35] Crunk AE, Monks J, Murakami A, Jackman M, Maclean PS, Ladinsky M, et al. Dynamic regulation of hepatic lipid droplet properties by diet. PLoS One 2013;8:e67631.
[36] Krahmer N, Najafi B, Schueder F, Quagliarini F, Steger M, Seitz S, et al. Organellar proteomics and phospho-proteomics reveal subcellular reorganization in diet-induced hepatic steatosis. Dev Cell 2018;47:205-21 e7.
[37] Khodayari N, Oshins R, Alli AA, Tuna KM, Holliday LS, Krotova K, et al. Modulation of calreticulin expression reveals a novel exosome-mediated mechanism of Z variant alpha1-antitrypsin disposal. J Biol Chem 2019;294:6240–52.
[38] Khodayari N, Marek G, Lu Y, Krotova K, Wang RL, Brantly M. Erdj3 has an essential role for Z variant alpha-1-antitrypsin degradation. J Cell Biochem 2017;118:3090–101.
[39] Ilhan A, Gartner W, Nabokikh A, Daneva T, Majdic O, Cohen G, et al. Localization and characterization of the novel protein encoded by C20orf3. Biochem J 2008;414:485–95.
[40] Albrektsen T, Richter HE, Clausen JT, Fleckner J. Identification of a novel integral plasma membrane protein induced during adipocyte differentiation. Biochem J 2001;359:393–402.
[41] Csaky Z, Garaiova M, Kodedova M, Valachovic M, Sychrova H, Hapala I. Squalene lipotoxicity in a lipid droplet-less yeast mutant is linked to plasma membrane dysfunction. Yeast 2020;37:45–62.
[42] Son SH, Park G, Lim J, Son CY, Oh SS, Lee JY. Chain flexibility of medicinal lipids determines their selective partitioning into lipid droplets. Nat Commun 2022;13:3612.
[43] Yoshioka H, Coates HW, Chua NK, Hashimoto Y, Brown AJ, Ohgane K. A key mammalian cholesterol synthesis enzyme, squalene monooxyge-

nase, is allosterically stabilized by its substrate. Proc Natl Acad Sci USA 2020;117:7150–8.
[44] Herrera-Marcos LV, Martinez-Beamonte R, Arnal C, Barranquero C, Puente-Lanzarote JJ, Herrero-Continente T, et al. Dietary squalene supplementation decreases triglyceride species and modifies phospholipid lipidomic profile in the liver of a porcine model of non-alcoholic steatohepatitis. J Nutr Biochem 2023;112:109207.
[45] Zhang L, Zeng J, Wu H, Tian H, Song D, Wu W, et al. Knockdown of TXNDC5 alleviates CCL4-induced hepatic fibrosis in mice by enhancing endoplasmic reticulum stress. Am J Med Sci 2023;366:449–57.
[46] Tilvis R, Kovanen PT, Miettinen TA. Metabolism of squalene in human fat cells. Demonstration of a two-pool system. J Biol Chem 1982;257:10300–5.